Journal of Materials Chemistry B

Accepted Manuscript

ROYAL SOCIETY OF CHEMISTRY

www.rsc.org/materialsB

Journal of
Materials Chemistry B

RSCPublishing

ARTICLE

An ESIPT fluorescent dye based on HBI with high quantum yield and large stokes shift for selective detection of Cys

Cite this: DOI: 10.1039/x0xx00000x

Received 00th January 2012,
Accepted 00th January 2012

DOI: 10.1039/x0xx00000x

www.rsc.org/

Ying Zhang,[a, b] Jun-Hao Wang,[b] Wenjie Zheng,[a] Tianfeng Chen,[a] Qing-Xiao Tong*[b] and Dan Li*[b]

We report 3-(4,5-diphenyl-1H-imidazol-2-yl)naphthalen-2-ol (**DPIN**) as an interesting luminescent material displaying ESIPT with large stokes shift (~180 nm) even in protic/polar solvent. Stable homo-dispersed nanoparticles caused by inter-and intramolecular H-bonds in aqueous media and corresponding aggregation induced enhanced emission with high quantum yield up to 0.45 were observed. Factors such as pH value and ions (cations and anions) showed negligible effect on the fluorescence performance. Probe of 3-(4,5-diphenyl-1H-imidazol-2-yl)naphthalen-2-yl acrylate (**DPIN-A**) based on this molecule was designed. The results revealed that it can be used for sensing of Cys with high selectivity and sensitivity.

1. Introduction

Molecules with excited-state intra-molecular proton transfer (ESIPT) have emerged as a class of promising luminescent materials in many practical applications, such as optical memories[1] and switches,[2] UV absorbers,[3] laser dyes,[4] radiation detection scintillators,[5] white light OLEDs[6] and particularly fluorescent probes.[7-18] ESIPT molecules can undergo a fast ($k \approx 10^{12}$ s^{-1}) photo-tautomerization reaction to yield an excited keto form (K*), mediated by an intra-molecular hydrogen bond (H-bond) upon photo-irradiation[19] (Scheme S1), which are famous for an abnormal emission with large stokes shift emission (100 nm ~ 200 nm) without self-absorption.

Among the reports on ESIPT molecules in probes design, derivatives of 2-(2-hydroxyphenyl) benzoxazole (**HBO**) and 2-(2-hydroxyphenyl) benzthiazole (**HBT**) are most attractive showing remarkable results with very high selectivity and sensitivity for detection of cellular transmembrane potential[7,8], apoptosis[9], Mg^{2+}[10], protein tyrosine[11], F^-[12,18], Cysteine and Homocysteine[13], Zn^{2+}[14,16,17] Pd^{2+}[15]. However, there are still some critical aspects that should be improved: i) ESIPT emissions are usually sensitive to protic/polar solvents[11, 20] and often inhibited with only normal emission (at much shorter wavelengths); and ii) Very low fluorescence quantum yields of 0.02 (for **HBO**) and 0.005 (for **HBT**).[19] All these problems have severely limited their applications in bio-sensing and bio-imaging.[21] Many efforts have been devoted to increase fluorescence quantum yields of these ESIPT molecules by introducing bulky dendrimer structures to inhibit the isomerization efficiency;[22] or by introducing moieties with H-bond for variation of inter- and intramolecular interactions to restrict molecular motions.[23, 26] On the other hand, aggregation induced enhanced emission (AIEE) fluorophores have shown distinct advantages in many areas of applications such as chemo/biosensors[24] and OLEDs.[25] ESIPT materials with AIEE properties have also been developed[23, 26] due to high quantum yields in aggregation states and avoidance of interactions with solvents. It is very important to generate such homo-dispersed aggregation nanoparticles in solution for detection applications. *Kim et al.* obtained organic nanoparticles in a poor solvent with almost exclusively the abnormal emission assigned to the keto tautomer.[11] However, the high critical concentration of the ESIPT molecules for the keto-emission results in a turbid solution, which is not favourable for the detection efficiency. *Yang, et al.* solved the above problem by dispersing the probes in CTAB micelle with smaller aggregates and consequently clear solution, in which high reactivity towards F^- was observed.[12] The probing media was further extended to pure

[a] Department of Chemistry, School of Life Science and Technology, Jinan University, Guangzhou 510632, China.
[b] Department of Chemistry and Research Institute for Biomedical and Advanced Materials, Shantou University, Guangdong 515063, China.
E-mail: qxtong@stu.edu.cn, dli@stu.edu.cn;

† Electronic Supplementary Information (ESI) available: Schematic representation of the ESIPT photocycle, synthetic routes of the **HBI**s and **HBO**s, and crystal data for **DPIN** (CCDC 983882). See DOI: 10.1039/b000000x/

water by dispersing an insoluble organic dye in PVP hydrogel substrates with enhanced sensing performance.[18] Although the advances are significant, the preparation of the detection systems is complicated and time-consuming. Thus, it is still of significance to develop new ESIPT dyes which can form homo-dispersed and stable nanoparticles in aqueous solution with more simplicity and higher quantum yields.

It is well known that **HBI**s (2-(2-hydroxyphenyl) benzimidazole derivatives) have much higher quantum yields than **HBO**s and **HBT**s.[19] Nevertheless, to the best of our knowledge, very few derivatives or analogues of **HBI** have been photophysically studied and rare fluorescent probes based on them have been reported by taking advantage of the ESIPT originated emission.[29] There are two drawbacks that hampered the development of **HBI**s displaying ESIPT emissions in probes design: i) the keto emission of classical **HBI**s locates mainly in the blue region (470 nm), which exhibited much smaller stokes shift compared with **HBO**s (500 nm) and **HBT**s (520 nm); ii), the potential interference from other cations or anions towards the binding-able site (NH, N=) of the imidazole ring would block intramolecular H-bonds involved in the ESIPT process, which severely reducing quantum yields of the ESIPT emission. In this work, we tried to modify the structure of **HBI** to improve the ESIPT emission performance by not only increasing its stokes shift but also quantum yields. With a simple one-pot reaction, we obtained **DPIN** (3-(4,5-diphenyl-1H-imidazol-2-yl)naphthalen-2-ol, Scheme 1). The compound exhibited obvious keto-form emission even in some polar and protic solvents (DMF, DCM and ethanol) at low concentration with large stokes shift and a high quantum yield up to 0.30 in DMF. Transparent solution can be obtained by dispersing **DPIN** in water in which stable homo-dispersed aggregated nanoparticles of **DPIN** were formed, showing almost exclusive keto-emission with a quantum yield of 0.20. The fluorescence stability of **DPIN** in water was also demonstrated by interference experiments involving factors such as pH value and ions (cations and anions).

An elevated level of biothiols (Cys, GSH and HCy) could bring out different diseases, however, they are difficult to be distinguished because of their similarity in structures.[28] For sensors displaying ESIPT, the signalling transduction is often achieved by the turn-on fluorescence of keto-form emission upon response to the analytes.[11-18] Based on the excellent fluorescence performance of **DPIN**, we designed a new probe denoted as **DPIN-A** (Scheme 1) by protecting the OH- moiety of **DPIN** with acryloyl group which can react with biohiols Cys selectively. The results show that **DPIN-A** has a high selectivity and sensitivity towards Cys in pure water which is of important significance in clinical diagnose.

2. Results and discussion

2.1 Design of HBIs and organic probe for Cys

DPIN was designed based on **HBI** with following considerations: i) **HBI**s have high fluorescent quantum yield about one order of magnitude higher than that of **HBO**s and **HBT**s; ii) The NH of the imidazole core as H-bonding donor would enhance intermolecular interaction which is beneficial for molecular aggregations; iii) The two phenyls as tails of imidazole with a large restricted angle for intermolecular π-π stacking, which is the main reason for aggregation caused fluorescent quenching; iv) Expanding the π-conjugation length by introducing 3-OH-2-naphthalene ring as the head of the molecule would result in a keto emission in longer wavelength with larger stokes shift, with which the distinct colour difference compared with normal emission would be discerned by naked eyes.

By protecting the OH- of **DPIN** with allyl group, we synthesized the probe **DPIN-A** (Scheme 1) with enol emission blocked due to the PET (Photoinduced Electron Transfer) process between the skeleton to the propylene moiety. After the conjugate addition of the three similar biothiols with the acrylates, it will generate thioethers which will interrupt the PET process with enol-like emission. It can further undergo an intramolecular cyclization to free the OH of **DPIN-A** which can undergo ESIPT process with keto emission (Scheme 1). **DPIN-A** was expected to have a high selectivity towards Cys over Hcy and GSH for the different intra-molecular cyclization rates.[13]

2.2 Synthesis and crystal structures

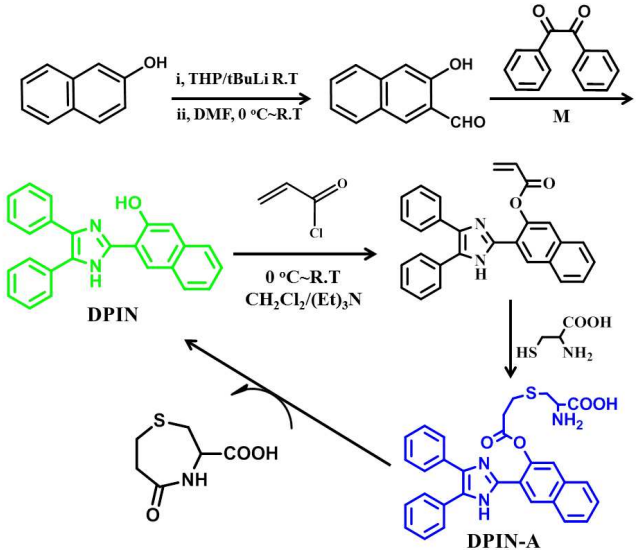

Scheme 1. Synthetic routes of DPIN and the target probe DPIN-A. And the reaction process of the probe towards Cys. (M: NH_4Ac/HAc/reflux.)

Synthetic routes of **DPIN** and the target probe are outlined in Scheme 1. Another four ESIPT dyes of **HPO-1**, **HPO-2**, **HPI-1** and **HPI-2** were synthesized for comparison (Scheme S2). **DPIN**, **HPO-1**, **HPO-2** were obtained by refluxing benzil/phenanthrene-9,10-dione, Ar-aldehyde, NH_4Ac in HAc as solvent. **HPI-1** and **HPI-2** were obtained by refluxing phenanthrene-9,10-dione, Ar-Aldehyde together in the mixed solvent of CH_2Cl_2/Ethanol, catalyzed by a small quantity of HAc in one pot reaction (for details, see experimental section). The resulting compounds were characterized by ^{1}H-NMR, Elemental analysis, and MS.

Single crystals of **DPIN** was obtained by layering hexane on CH_2Cl_2. X-ray single-crystal diffraction analysis revealed that **DPIN** crystalized in a triclinic, p-1 group. As shown in Fig. 1, three different kinds of weak interactions were observed: i) the short distance of 1.7 Å between H and N indicated strong intramolecular O-H···N hydrogen bonds, which favours the mobility of proton from -OH to Lewis base =N sites in the imidazole centre. ii) Intermolecular N-H···O hydrogen bond with distance of 2.0 Å and iii) Intermolecular C-H···π interactions within distance of 3.08~3.29 Å are beneficial for the molecular aggregation in the solution with a high concentration and insoluble solvent. As expected, the intermolecular π-π stacking was suppressed due to the large twisted dihedral angle between the phenyl and imidazole rings (ca. 51.87º or 43.97º). The crystal stacking was shown in Fig. S1. Selected dihydral angles and weak interactions were given in Table S1. Structural parameters and data were listed in Tables S2 and S3.

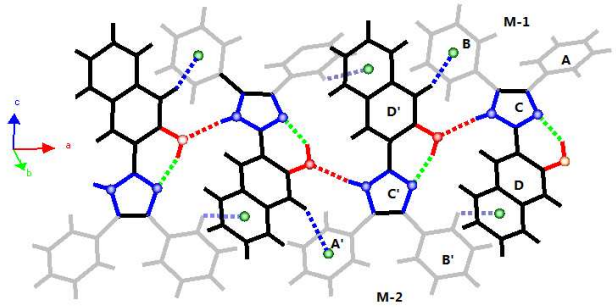

Fig. 1. Crystal packing structure of DPIN, dot lines represent weak intermolecular interactions: O-H···N (green), N-H···O (red), C-H···π (blue).

2.3 Emission of HBIs

Strong keto emission with large stokes shift in polar/protic solvent are important for ESIPT molecules. As given in Fig. 2, **DPIN** exhibited strong keto emissions (maximized at >540nm) with large stokes shifts in normal strong polar and protic solvents, except that in methanol. Different colours were observed from blue, green, yellow and red under the radiation under a UV lamp with 365 nm, due to different ratios between keto and enol emissions in different solutions. The bathochromic-shift of the keto-form emission in different solvents (553, 610 nm in DMF and cyclohexane, respectively) is well in accordance with the n-π* transition character of the keto tautomer. However, at a low concentration of 10 μM, the enol emission at ~415 nm is very weak, while the keto emission is strong with large stokes shift peaked at ~553 nm even in polar (DMF) and protic solvents (ethanol) with yellow and green emissions, respectively. In nonpolar solvents the emissions show orange yellow at ~600 nm for benzene and DCM and red (~610 nm) for cyclohexane. To elucidate the origination of the excellent fluorescence performance of **DPIN**, emission spectra of four other molecules with similar structures (**HPO-1**, **HPO-2**, **HPI-1** and **HPI-2**) were also characterized and given in Fig. S2. The emissions of **HPO-1** and **HPO-2** showed much larger dependence than **HPI-1**, **HPI-2** and **DPIN** on solvents with just moderate keto-form emission in non-polar solvents. After careful examination of their structures, we deduce that the less dependence on solvents of the keto-emission of **DPIN** and **HPI-1** and **HPI-2** might be mainly attributed to the molecular aggregation due to the presence of NH- within imidazole ring which can act as hydrogen donor for intermolecular H-bonding interactions. **HPO-1**, **HPO-2**, **HPI-1** and **HPI-2** showed smaller stokes shift than **DPIN** in spite of the involvement of more conjugated 9,10-phenanthrenequinone instead of benzil as the tail of these molecules. It has been demonstrated that the highest occupied molecular orbitals (HOMO) of the keto form of **HPI** are mainly located at the imidazole ring and the head substituents in which extending their conjugation length can reduce the energy gap efficiently.[6] The introduction of 3-OH-2-naphthalene as the head of **DPIN** is essential to the large stokes shift of the keto-emission for its longer conjugation length than 2-OH-naphtanlene and benzene. These results prove that the NH- in the imidazole ring and the 3-OH-2-naphthalene are crucial for the stable keto emission with large stokes shift. Compared with other ESIPT molecules, the excitation and emission of **DPIN** at longer wavelength (ex, ~371 nm; enol emission, ~415 nm; keto emission, ~550 nm) are much more beneficial for biosensing and bioimiaging.[11-18]

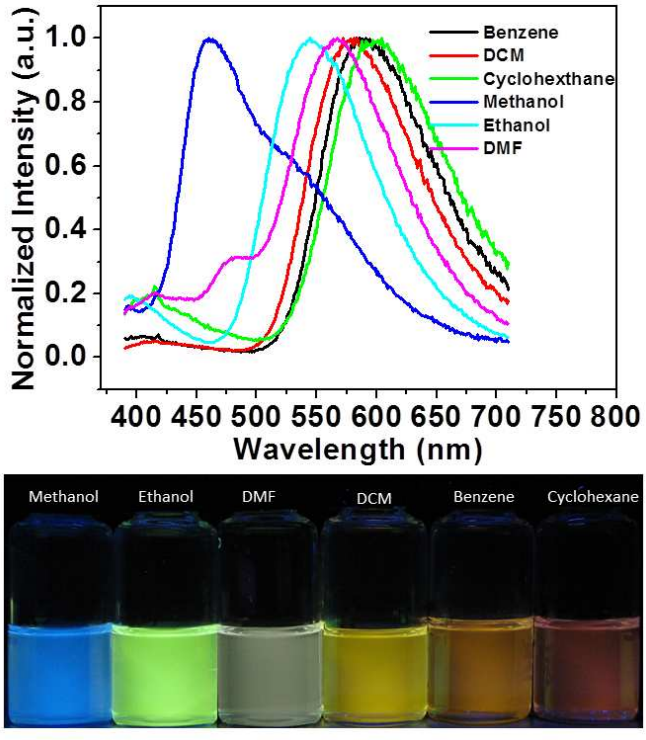

Fig. 2. Fluorescent of DPIN (10 μM) in different solvents excited at 371 nm (top); Pictures of DPIN in different solvents (10 μM) excited with hand lamp at 365 nm (Down).

2.4 Emission performance of DPIN in DMF with different concentrations

Many organic dyes suffer aggregation caused quenching (ACQ) in concentrated solution or solid states for the π-π stacking. To

avoid ACQ, we introduced benzil with large twisted angles into **DPIN**. As shown in Fig. 3, the fluorescent spectra at low concentration of 2.5 μM in DMF mainly at ~480 nm which originated from the species resulting from the interaction of solvent with **DPIN**. Two shoulders at 415 nm and 565 nm can be assigned to enol emission and keto emission, respectively according to previous reports. Upon increasing the concentration from 2.5 μM to 100 μM, the intensity of keto emission mainly at 565 nm appears and increases rapidly. This was further demonstrated by the colour change discerned by naked eyes from blue (2.5 μM), yellow (10 μM) to bright yellow (50 μM) under 365 nm radiation (Fig.3 Inset). This enhanced keto tautomer emission can be attributed to the increased planarity and rigidity between imidazole and naphthalene rings as well as the restriction of molecular motion by the J-aggregation with a head-to-tail arrangement which is more facile for the tautomerization of **DPIN** from enol-form to keto-form upon photo excitation.[18, 23]

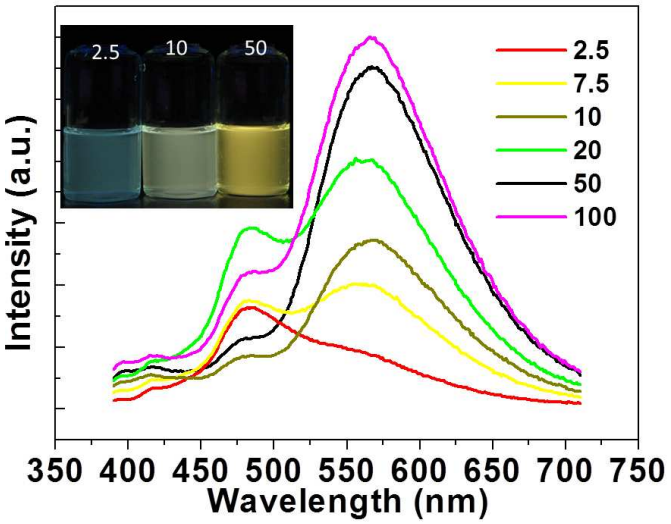

Fig. 3. PL of DPIN in DMF with different concentration ranging from 2.5 μM to 100 μM under 371 nm excitation. Inset picture: Emission colour of DPIN in DMF with different concentration, excited under 365 nm hand lamp.

2.5 Effect of H_2O fraction on Emission performance

We also investigated addition of H_2O on the fluorescence performance of **DPIN** in DMF solution (10 μM). The fluorescence spectra showed obvious change upon increasing the ratio of H_2O from 0 to 100% (Fig. 4a). Similar fluorescent performance of **DPIN** in THF with different H_2O proportion is shown in Fig. S3. In pure DMF, beside the strong keto-form emission at *ca.* 565 nm and weak enol-form emission at *ca.* 415 nm, the emission spectra of **DPIN** displayed a third weak peak at ca. 480 nm which might be due to the formation of species that are intermolecularly hydrogen-bonded to DMF molecules. Upon addition of water, this peak disappeared and the intensity of enol-form emission increases upon the concentration of H_2O up to 70% while the keto-form emission showed irregular change. The decreasing intensity ratio between the keto- and enol-form emissions below addition of water up to 80% may be due to the formation of hydrogen bond between **DPIN** and water which is an obstacle for the tautomerization of **DPIN** from enol to keto form. The keto-form emission becomes more prominent until the concentration up to 90% which may be the critical concentration for the aggregation of **DPIN** to nanoparticles (Fig. 4b). Only keto-form emission can be observed in 100% water which can be attributed to the formation of nanoparticles. Consequently, the emission colour can be varied from yellowish green (0%), yellow (60%) to green (100%) with different water content, which are in well accordance with the spectral change (Fig. 4a inset). DLS analysis (Dynamic Light Scattering) (Fig. 4c) showed that the size of the nanoparticles is about 205 nm in pure water. The formed solution is stable which is still clear after standing for 12 h with negligible change in the emission spectra (Fig. S4).

The absolute quantum yields of keto-emission of **DPIN** in DMF, pure water and DMF/H_2O mixed solution (10 μM, *v:v*, 2:3) were measured by using integrating sphere. It shows high quantum yields of 0.30 (keto emission quantum yield: 0.28), 0.45 (keto emission quantum yield: 0.39), and 0.20 in DMF, DMF: H_2O (2:3) and pure water, respectively. These are much higher than that of reported AIEE ESIPT molecules.[23]

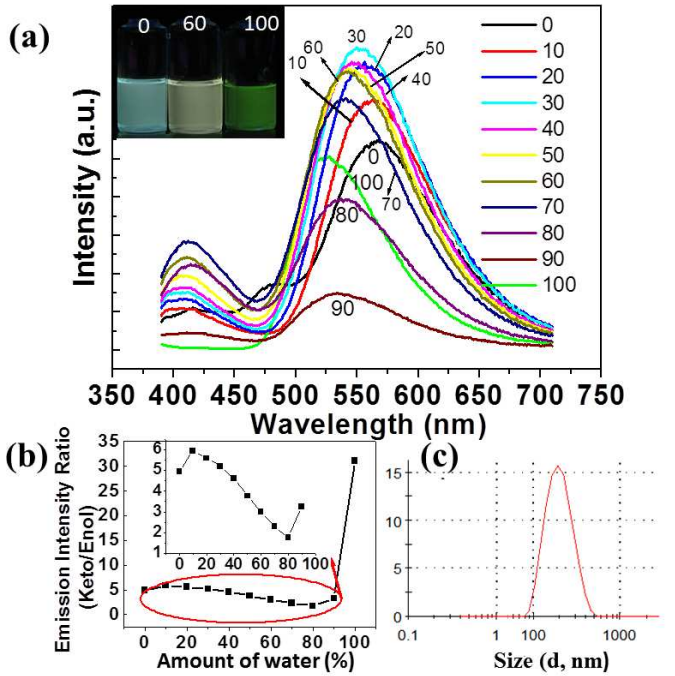

Fig. 4. (a), Fluorescent of DPIN in DMF and H_2O mixed solution (10 μM), with proportion of H_2O increasing from 0 to 100% water v/v in DMF. Excited wavelength : 371 nm. Inset picture: fluorescence of DPIN solution with different content of H_2O, excited under 365 nm hand lamp. (b), Ratio of intensity of keo emission toward enol emission. (c), Size distribution of DPIN in pure water by DLS.

2.6 pH effects

As known, **HBI**s have amphoteric property due to the presence of both Lewis acidic –NH- and basic =N- sites in the imidazole ring. It is very important to examine the pH effect on the fluorescence performance of **DPIN**. The experiments were conducted in PBS buffer (20 mM). The results showed that the performance of the fluorescence of **DPIN** hardly changed under different pH values from 6.0 to 8.8 (Fig. 5a). The experiment results indicate that **DPIN** is a good candidate dye displaying ESIPT for application in physiology environment.

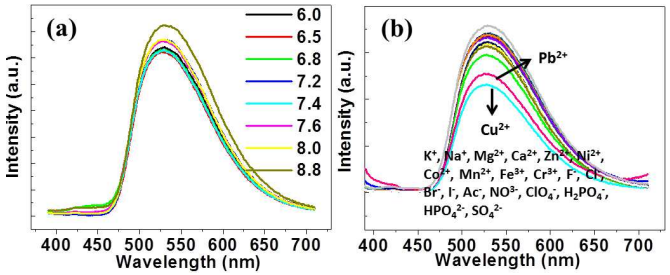

Fig. 5. The fluorescent spectra of DPIN (10 μM) in PBS buffer (20 mM, pH, 7.2) : (a) with pH from 6.0 to 8.8; (b) with common cation and ions (100 eq.) added.

2.7 Interference of common ions

Imidazole behaves as not only an excellent hydrogen bond donor to anion receptor but also electron donor that can bind metal ions by coordination bonds. In other words, the fluorescence of dyes involving imidazole rings may be affected profoundly by the presence of ions.[27] On this account, it is necessary to investigate the effect of ions on the fluorescence performance of **DPIN**. The experiments were carried out in PBS buffer (20 mM, PH, 7.2) with common cations and anions. As shown in Fig. 5b, all the ions examined showed negligible effect on the intensity of the emissions. It is concluded that the fluorescence performance of **DPIN** would not be disturbed by common ions.

2.8 Optical responses of probe DPIN-A towards Cys

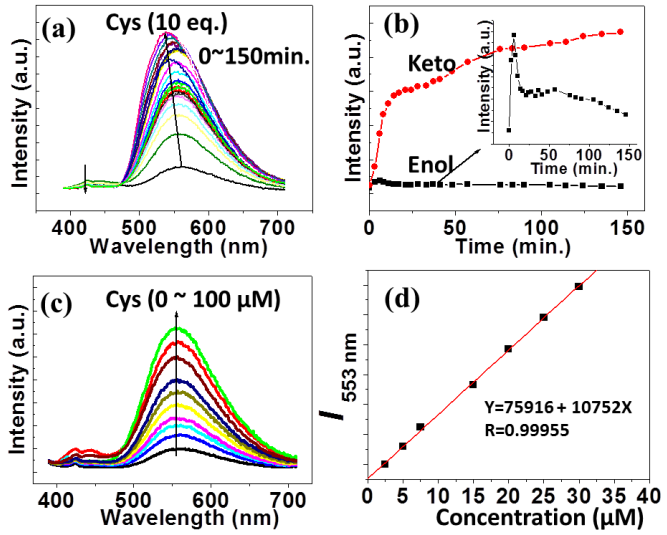

Fig. 6. (a) The fluorescent spectra of DPIN-A (10 μM) in PBS buffer (20 mM, PH, 7.2) in the presence of 10eq. Cys from 0 to 150 min. (b) The fluorescent emission intensity for keto emission (λ=553 nm) and enol emission (λ=425 nm) as time increasing. (c) The fluorescent spectra of keto emission in the presence of different amounts of Cys after 30 min. (d) The fluorescent intensity at 553 nm toward different amounts of Cys from 0~30 μM.

In view of the excellent fluorescence performance of **DPIN**, we designed a new probe **DPIN-A** for Cys by protecting the -OH group with allyl group. The formed acrylate quenched both the enol- and keto-form emissions due to the PET process and block of the –OH group. Condensation of acrylates with Cys which could release the –OH group in two step reactions restored the **DPIN** emission. This fluorescent turn-on process had been reported to detect Cys in CTAB micelle with obvious color change discerned by eyes.[12] Here, we investigated the sensing performance for Cys of **DPIN-A** in a more simple protocol. The experiments were carried out using a 10 μM solution of **DPIN-A** in pure water (PBS buffer, 20 mM, pH, 7.2). Fig. 6a shows the fluorescent spectra of the assay system in the presence of Cys (10 eq.) for 150 min. After the addition of Cys, the intensity of keto-form emission increases gradually, while that of enol-form emission increased quickly at first (~10 min.) then decreased gradually. The emission intensity keeps relatively stable in about 20 minutes for both enol- and keto-emission (Fig. 6b). The enol emission increases initially due to the conjugate addition which removes the alkene-induced PET quenching and the increase of the keto emission is due to the formation of lactam releasing **DPIN** exhibiting ESIPT process.

We also investigated the fluorescent response of **DPIN-A** towards different amounts of Cys (0 ~ 100 μM) after reaction for 30 min. The results (Fig. 6c) showed that the increasing intensity of the major peak at ca. 553 nm correlates with the increasing concentration of Cys. The Intensity *vs.* concentration of Cys plot shows linear correlation to the amounts of Cys from 0 to 30 μM (Fig. 6d). The detection limit of Cys was calculated to be 0.21 μM which is below the requisite detection limits for Cys assays,[30] indicating that **DPIN-A** is suitable for sensing Cys with good sensibility in pure water.

2.9 Selective detection of biothiols

To evaluate the selectivity of **DPIN-A** towards Cys, we studied the fluorescence performance of **DPIN-A** responding to biothiols (10 eq.) and other amino acids (100 eq.) in pure water (PBS buffer, 20 mM, pH, 7.2). The emission spectra changed slightly compared with the blank sample in the presence of other 19 kinds of amino acids, indicating that the other amino acids did not react with **DPIN-A**. Biothiols including Hcy, Cys and GSH have similar structures which just differ by a single methylene unit in their side chains.[28] It can be seen that (Fig. 6b, Fig. 7a) all of them can give rise to enol emission (λ = 425 nm) indicating their conjugate addition reactions with **DPIN-A**. Interestingly, only the addition of Cys can significantly increase the intensity ratio between the keto- and enol-form emissions. It displays strong emission at ~553 nm while the enol emission peaked at ~425 nm is very weak. The emission intensity change of **DPIN-A** towards Hcy and GSH with time were shown in Fig. S5. Compared with Cys, the emission at 425 nm for Hcy and GSH was much stronger than that of Cys, indicating they cannot be removed quickly after conjugation with **DPIN-A**. The high selectivity of Cys over Hcy and GSH was further proved by the ratio between emission intensity at 553 nm and 425 nm as time increasing (Fig.7b). For Cys, it reached the stable ratio about 12 after 20 min. with yellowish-green emission, whereas HCy and GSH show much lower ratio (below 2.0) with blue emission (Fig.7b **inset**). In Fig.7c we can directly see that the emission intensity ratio of keto *vs.* enol is high up to ~14 towards Cys of **DPIN-A** after reaction for 30 min. It has a higher selectivity over other amino acids and

biothiols which exhibits a ratio below ~2.0 even after a longer reaction time of 1 h.

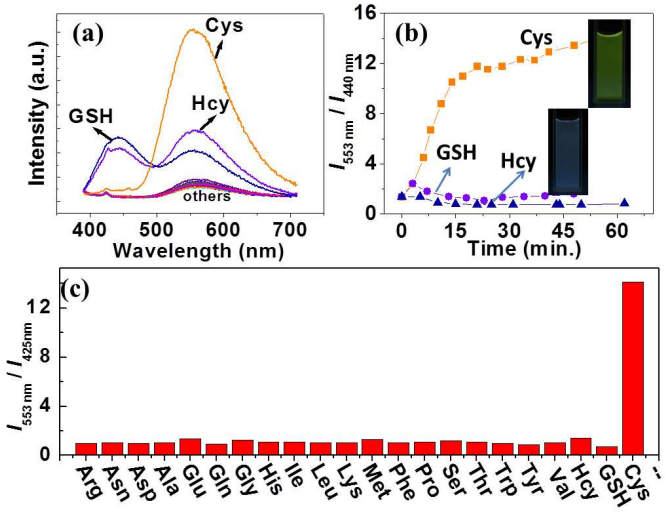

Fig.7. (a) Fluorescent spectra of DPIN-A (10 μM) towards Cys (10 eq.), Hcy, (10 eq.) GHS (10 eq.) . The spectra were recorded after 30 min. Other amino acids (100eq. obtained after 1 hour.) (b) The ratio of fluorescent intensity centred at 553 nm and 425 nm towards Cys, Hcy and GSH with a function of time. (c) Intensity ratio (of Keto emission and enol emission) of the probe (10 μM) towards other amino acids (100 eq., data was obtained after 1 hour) and biothiols of Hcy, GSH and Cys (10 eq., data was obtained after 30 min.)

2.10 Interference experiment

To further investigate the selectivity of Cys over other competitive species, interference experiments of other amino acids towards Cys were carried out. The intensity ratio between 553 nm and 425 nm of the probe (Fig. 8) displays no distinct change after being cultured with excessive other amino acids (100 eq.) for about one hour (red bars). Upon addition of 10 eq. Cys in the buffer solution of **DPIN-A** together with other amino acids (100 eq.) for about an hour, the intensity ratio increased significantly (green bars), indicating that **DPIN-A** can selectively detect Cys without interference from other amino acids.

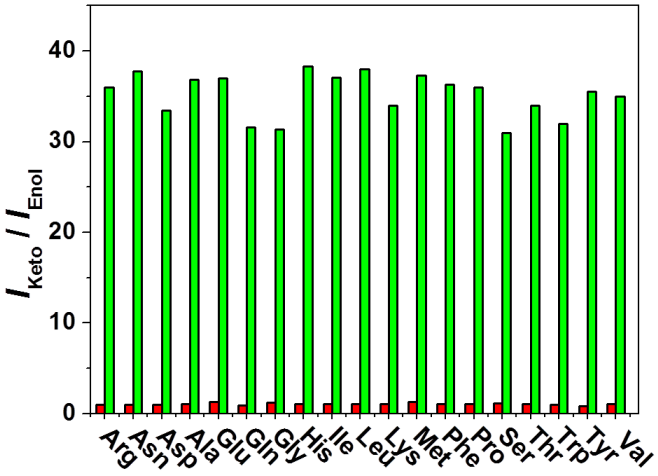

Fig.8. Bars represent the final fluorescence intensity at 528nm in PBS buffer (20 mM, pH, 7.2). Red bars: Emission responses of DPIN-A towards amino acids (100eq.). Green bars: Emission responses of DPIN-A (10 μM) towards amino acids (100eq.) (100 eq.) in the presence of Cys (10 eq.) All the data was obtained after 1h.

3. Experimental section

Materials and general methods

^{1}H-NMR spectra were recorded on a Varian Gemin-400 MHz spectrometer. Fluorescence spectra and absolute quantum yields (measured with an integrating sphere) were measured on an optical spectrometer (PTI: QM-TM, USA). MS analyses were recorded on Perkin Elemer Flexar SQ 3000 mass spectrometer. Elemental analysis (C, H and N) was performed using a Vario EL III CHNS elemental analyzer. Single crystal structure of **DPIN** was obtained by X-ray diffraction with a Gemini A Ultra X-ray single crystal diffractometer using graphite monochromatized Cu-Kα radiation (Cu-Kα, λ= 1.54184 Å). All pH measurements were made with a Sartorius (PB-10) pH meter. Dynamic Light Scattering (DLS) measurement was performed on nano Zetasizer (Malvern). Flash chromatography was per-formed with silica gel (200–300 mesh). Spectroscopic grade DMF and MilliQ water, (18.2 MΩ cm, 25 ºC) were used throughout the detection experiments.

Synthesis of 3-hydroxy-2-naphthaldehyde

3-Hydroxy-2-naphthaldehyde was synthesized according to the previous reported literature with little modification.[31] In a dry 100 mL round bottom flask was typically charged with 6 mmol of the naphthalen-2-ol, dissolved in 3 mL of anhydrous THP under N_2 protection. Then 5.6 mmol of 1.6 M *t*-BuLi in pentane was added dropwise via a syringe in approximately 2 min to the stirred solution at room temperature. Immediately a rapid evolution of heat and gases occurred, thus raising the temperature of the reaction mixture to *ca.* 50 ºC. After the gas evolution subsided (15 min.), the reaction mixture was left to stir for another 4 h. A solution of the DMF (3 mL) in THP (3 mL) was then added to the above mixture at the 0 ºC and, subsequently left to stir for 24 h at room temperature. After the reaction finished, add water carefully to the mixture and drop 1 M HCl until pH was 5~6. The mixture was extracted with ethyl acetate, dried over anhydrous Na_2SO_4 and evaporated to dryness. The resulting residue was chromatographed on silica gel (Petroleum Ether:CH_2Cl_2, 3:1), a bright yellow powder was then obtained with 60% yield. ^{1}H NMR (400 MHz, DMSO) δ 7.30 (s, 1H), 7.36 (ddd, 1H), 7.55 (ddd, 1H), 7.77 (d, 1H), 7.99 (d, 1H), 8.36 (s, 1H), 10.42 (s, 1H), 10.59 (s, 1H).

Synthesis of 3-(4,5-diphenyl-1*H*-imidazol-2-yl)naphthalen-2-ol (DPIN) (1)

The product was prepared by refluxing benzil (0.21 g, 1 mmol), 3-hydroxy-2-naphthaldehyde (0.32 g, 1.2 mmol) and ammonium acetate (0.75 g, 10 mmol) in glacial acetic acid (50 mL) for 24 h under an argon atmosphere. After cooling to room temperature, a pale yellow mixture was obtained and poured into a methanol solution under stirring. The separated solid was filtered off, washed with methanol, and dried to give a light yellow solid. The solid was purified by column chromatography (Petroleum Ether: CH_2Cl_2, 1:1) on silica gel. ^{1}H NMR (400 MHz, DMSO-d6, TMS) δ 5.32 (d, J = 4.7 Hz, 1H), 7.19-7.67 (m, 12H), 7.78 (dd, J = 18.1, 8.0 Hz, 2H), 8.66

(s, 1H), 12.93 (s, 1H), 13.32 (s, 1H). MS (ESI): m/z Calculated 362.46, found 362.76. Anal. Found: C, 82.36; H, 5.08; N, 7.45. Calc. for $C_{25}H_{18}N_2O$: C, 82.85; H, 5.01; N, 7.73%.

2-(phenanthro[9,10-*d*]oxazol-2-yl)phenol (HPO-1)

HPO-1 was synthesized using a similar approach for DPIN. ^{1}H NMR (400 MHz, DMSO) δ, 7.17 (ddd, J = 15.1, 8.3, 4.3 Hz, 2H).7.41 – 7.66 (m, 1H), 7.73 – 7.99 (m, 4H), 8.25 (dd, J = 7.8, 1.5 Hz, 1H), 8.44 (dd, J = 7.9, 1.1 Hz, 1H), 8.58 (dd, J = 7.8, 1.2 Hz, 1H), 9.01 (t, J = 8.6 Hz, 2H), 11.17 (s, 1H). MS (ESI): m/z Calculated 311.33, found 311.46. Anal. Found: C, 80.94; H, 4.43; N, 4.31. Calc. for $C_{21}H_{13}NO_2$: C, 81.01; H, 4.21; N, 4.50%.

2-(1*H*-phenanthro [9,10-*d*]imidazol-2-yl)phenol (HPI-1)

9,10-phenanthrenequinone (2.12 g, 10 mmol), ammonium acetate (0.75 g, 10 mmol) were added to the 30 mL mixed solvent of ethanol and dichloromethane (1:1, v/v). After refluxing for 10 min, Salicylaldehyde (0.32 g, 1.2 mmol) and a catalyst amount of glacial acetic acid were added. The reaction mixture was held at reflux for another 3 h. After cooling to room temperature, the mixture was filtered. The solid was purified by column chromatography (Petroleum Ether: CH_2Cl_2, 1:1) on silica gel. A white powder was finally obtained after it was stirred in refluxing ethanol, subsequently filtered, and dried in vacuum. ^{1}H NMR (400 MHz, DMSO) δ 5.32 (s, 1H), 7.09 (ddd, J = 4.5, 3.5, 1.8 Hz, 2H), 7.47 – 7.28 (m, 1H), 7.90 – 7.57 (m, 3H), 8.26 (dd, J = 8.1, 1.6 Hz, 1H), 8.56 (dd, J = 40.9, 7.7 Hz, 2H), 13.70 (s, 1H), 8.91 (dd, J = 12.7, 8.3 Hz, 2H), 13.14 (s, 1H). MS (ESI): *m/z* Calculated 310.35, found 310.70. Anal. Found: C, 81.16; H, 4.76; N, 8.94. Calc. for $C_{21}H_{14}N_2O$: C, 81.27; H, 4.55; N, 9.03%.

1-(phenanthro[9,10-*d*]oxazol-2-yl)naphthalen-2-ol (HPO-2)

HPO-2 was synthesized using a similar approach for DPIN. ^{1}H NMR (400 MHz, DMSO) δ 7.42 (d, J = 9.0 Hz, 1H), 7.48 (t, J = 7.4 Hz, 1H), 7.63-7.75 (m, 1H), 7.77-7.93 (m, 3H), 8.00 (d, J = 7.4 Hz, 1H), 8.12 (d, J = 9.0 Hz, 1H), 8.44 (d, J = 7.7 Hz, 1H), 8.56 (dd, J = 11.4, 8.4 Hz, 2H), 9.04 (t, J = 8.6 Hz, 3H), 11.91 (s, 1H). MS (ESI): *m/z* Calculated 361.39, found 361.75. Anal. Found: C, 82.95; H, 4.65; N, 3.98. Calc. for $C_{25}H_{15}NO_2$: C, 83.09; H, 4.18; N, 3.88%.

1-(1*H*-phenanthro[9,10-*d*]imidazol-2-yl)naphthalen-2-ol (HPI-2)

HPI-2 was synthesized using a similar approach for HPI-1. ^{1}H NMR (400 MHz, DMSO) δ5.32 (d, J = 4.3 Hz, 1H), 7.26 -7.44(m, 7H), 7.46 -7.52 (m, 1H), 7.52-7.62 (m, 4H), 7.88 (t, J = 8.5 Hz, 2H), 8.19 (d, J = 8.6 Hz, 1H). MS (ESI): *m/z* Calculated 360.41, found 360.42. Anal. Found: C, 83.60; H, 4.53; N, 7.85. Calc. for $C_{25}H_{16}N_2O$: C, 83.31; H, 4.47; N, 7.77%.

Synthesis of 3-(4,5-diphenyl-1*H*-imidazol-2-yl)naphthalen-2-yl acrylate (DPIN-A)

DPIN-A was obtained according to the reported literature.[15] To a solution of DPIN (182 mg, 0.5mmol) and Et_3N (2 eq) in 10 mL of anhydrous CH_2Cl_2, acryloyl chloride (1.25 eq, mixed with 4 mL of CH_2Cl_2) was added dropwise at 0 ºC. After stirring at this temperature for 90 min, the mixture was warmed to room temperature and stirred overnight. The solvent was removed in vacuum to furnish a crude mixture which afforded DPIN-A upon flash chromatography as a light orange solid (110 mg, 51% yield) ^{1}H NMR (400 MHz, DMSO) δ5.32 (s, 1H), 5.88 (s, 1H), 5.98-6.31 (m, 1H), 6.41-6.77 (m, 2H), 6.92-7.81 (m, 10H), 7.75-8.15 (m, 3H), 8.59 (s, 1H), 12.76 (s, 1H). MS (ESI): m/z Calculated 416.47, found 416.81. Anal. Found: C, 80.30; H, 4.90; N, 6.35. Calc. for $C_{28}H_{20}N_2O_2$: C, 80.75; H, 4.84; N, 6.73%.

4. Conclusion

In summary, by introducing benzyl as the tail, imidazole as the core and 3-OH-2-naphthalene as the head, we successfully designed and obtained an interesting ESIPT chromophore named **DPIN** which showed prominent ESIPT emission in protic and polar solvents with large stokes shift and high quantum yields. The benzyl tail with large twisted angle avoided aggregation induced quenching by restricting the intermolecular π-π stacking. The imidazole core supplies intermolecular H-bond sites which are in favour of J-aggregation in solution and ensure the prominent keto-form emission in protic and polar solvents. The 3-OH-2-naphthalene as the head of **DPIN** can extend the conjugation length effectively which results in a keto-emission with large stokes shift.

DPIN can be dispersed in water forming stable transparent solution with almost exclusively keto-form emission and high fluorescence quantum yield up to 0.20. The fluorescence performance is very stable in the physiology pH range of 6.2~9.2 and can't be interfered by other common ions.

The new turn-on sensor denoted as **DPIN-A** (Scheme 1) by protecting the OH- moiety of **DPIN** with acryloyl group showed high selectivity and sensitivity towards Cys and can discriminate Cys from other amino acids including GSH and Hcy in pure water. Further Studies are underway to optimize the sensing method.

Acknowledgements

This work was financially supported by the National Basic Research Program of China (973 Program, No. 2013CB834803), the National Science Foundation for Distinguished Young Scholars of China (No. 20825102) and the National Natural Science Foundation of China (Nos. 91222202, 21171114).

References

1. X. Chang, G. Tang, G. Zhang, Y. Liu, W. Chen, B. Yang, X. Zhang, *J. Opt. Soc. Am. B*, 1998, **15**, 854.
2. S. J. Lim, J. Seo, and S. Y. Park, *J. Am. Chem. Soc.* 2006, **128**, 14542 -14547.
3. J. Keck, H. E. A. Kramer, H. Port, T. Hirsch, P. Fischer, and G.

Rytz *J. Phys. Chem.*, 1996, **100**, 14468–14475.
4. (a) J. C. del Valle, R. M. Claramunt, J. Catalan, *J. Phys. Chem. A*, 2008, **112**, 5555-5565; (b) K. Y. Chen, C. C. Hsieh, Y. M. Cheng, C. H. Lai, P. T. Chou, *Chem. Commun.* 2006, 4395-4397; (c) K. I. Sakai, M. Ichikawa, Y. Taniguchi, *Chem. Phys. Lett.* 2006, **420**, 405-409.
5. M. L. Martinez, W. C. cooper, P. T. Chou, *Chem. Phys. Lett.* 1992, **193**, 151-154.
6. J. E. Kwon, S. Park, and S. Y. Park, *J. Am. Chem. Soc.* 2013, **135**, 11239-11246.
7. S. Andrey, A. P. D. Klymchenko, *J. Am. Chem. Soc.* 2002, **124**, 12372-12379.
8. A. S. Klymchenko, H. Stoeckel, K. Takeda, Y. Mely, *J. Phys. Chem. B*, 2006, **110**, 13624-13632.
9. V. V. Shynkar, A. S. Klymchenko, C. Kunzelmann, G. Duportail, C. D. Muller, A. P. Demchenko, J. M. Freyssinet, Y. Mely, *J. Am. Chem. Soc.* 2007, **129**, 2187-2193.
10. N. Singh, N. Kaur, R. C. Mulrooney, J. F. Callan,*Tetrahedron Lett.* 2008, **49**, 6690.
11. T. Kim, H. J. Kang, G. H. Sang, J. Chung and Y. Kim, *Chem. Commun.*, 2009, 5895–5897.
12. R. Hu, J. Feng, D. Hu, S. Wang, S. Li, Y. Li and G. Q. Yang, *Angew. Chem. Int. Ed.*, 2010, **49**, 4915 –4918.
13. X. Yang, Y. Guo and R. M. Strongin, *Angew. Chem. Int. Ed.* 2011, **50**, 10690 –10693.
14. W. Chen,Y. Xing and Y. Pang, *Org. Lett*., 2011**, 13,** 1362–1365.
15. B. Liu, H. Wang, T. Wang, Y. Bao, F. Du, J. Tian, Q. Li and R. Bai, *Chem. Commun.*, 2012, **48**, 2867–2869.
16. J. Wang, Q. Chu, X. Liu, C. Wesdemiotis, and Y. Pang, *J. Phys. Chem. B,* 2013, **117**, 4127 – 4133.
17. Y. Shiraishi, Y. Matsunaga and T. Hirai, *J. Phys. Chem. A,* 2013, **117**, 3387 – 3395.
18. L. Xiong, J. Feng, R. Hu, S. Wang, S. Li, Y. Li and G. Q. Yang, *Anal. Chem*. 2013, **85**, 4113− 4119.
19. K. Das, N. Sarkar, A. K. Ghosh, D. Majumdar, D. N. Nath and K. Bhattacharyya, J. Phys. Chem. 1994, **98**, 9126-9132.
20. J. Seo, S. Kim and S. Y. Park, *J. Am. Chem. Soc.*, 2004, **126**, 11154–11155.
21. J. Zhao, S. Ji, Y. Chen, H. Guo and P. Yang, *Phys. Chem. Chem. Phys.*, 2012, **14**, 8803–8817.
22. A. Ohshima, A. Momotake, R. Nagahata and T. Arai, *J. Phys. Chem. A,* 2005, **109**, 9731-9736.
23. Y. Qian, S. Li, G. Zhang, Q. Wang, S. Wang, H. Xu, C. Li, Y. Li and G. Q. Yang, *J. Phys. Chem. B,* 2007, **111**, 5861-5868.
24. (a) K. E. Achyuthan, L. Lu, G. P. Lopezc, D. G. Whitten, *Photochem. Photobiol. Sci.* 2006, **5**, 931-937; (b) O. K. Kim, J. Je, G. Jernigan, L. Buckley, D. Whitten, *J. Am. Chem. Soc.* 2006, **128** , 510-516; (c) Z. Zhou, Y. Tang, D. G. Whitten, K. E. Achyuthan, *ACS Appl. Mater. Interfaces*, 2009, **1**, 162-170; (d) M. Wang, G. Zhang, D. Zhang, D. Zhu, B. Z. Tang, *J. Mater. Chem.* 2010, **20**, 1858-1867; (e) W. Xue, G. Zhang, D. Zhang, D. Zhu, *Org Lett*. 2010, **12**, 2274-2277; (f) Y. Liu, C. Deng, L. Tang, A. Qin, R. Hu, J. Z. Sun, B. Z. Tang, *J. Am. Chem. Soc*. 2011, **133**, 660-663; (g) J. Wu, W. Liu, J. Ge, H. Zhang, P. Wang, *Chem. Soc.Rev*. 2011, **40**, 3483-3495. (h) P. S. Salinia, M. G. Derry Holadaya, M. L. P. Reddyb, C. H. Suresh and A. Srinivasan *Chem. Commun.* 2013, **49**, 2213-2215.
25. (a) Z. Ning, Z. Chen, Q. Zhang, Y. Yan, S. Qian, Y. Cao, H. Tian, *Adv. Funct. Mater.* 2007, **17**, 3799-3807; (c) Z. Zhao, S. Chen, C. Deng, J. W. Y. Lam, C. Y. K. Chan, P. Lu, Z. Wang, B. Hu, X. Chen, H. S. Kwok, Y. Ma, H. Qiu, B. Z. Tang, *J. Mater. Chem*. 2011, **21**, 10949-10956.
26. T. Iijima, A. Momotake, Y. Shinohara, T. Sato, Y. Nishimura, and T. Arai, *J. Phys. Chem. A,* 2010, **114**, 1603–1609
27. K. Skonieczny, A. I. Ciuciu, E. M. Nichols, V. Hugues, M. B. Desce, L. Flamigni and D. T. Gryko, *J. Mater. Chem*., 2012, **22**, 20649-20664.
28. G.-L. Liu, D.-Q. Feng, X.-Y. Mu, W.-J. Zheng, T.-F. Chen, L. Qi and D. Li, *J. Mater. Chem. B* , 2013, **1**, 2128-2131.
29. P. Molina, A. Tárraga and F. Otón, *Org. Biomol. Chem.*, 2012, **10**, 1711-1724.
30. O. Rusin, N. N. S. Luce, R. A. Agbaria, J. O. Escobedo, S. Jiang, I. M. Warner, F. B. Dawan, K. Lian, R. M. Strongin, *J. Am. Chem. Soc.* 2004, **126**, 438 – 439;
31. G. Coll, J. Morey, A. Costa, and J. M. Saa, *J. Org. Chem.* 1988, **53**, 5345-5348.

TOC

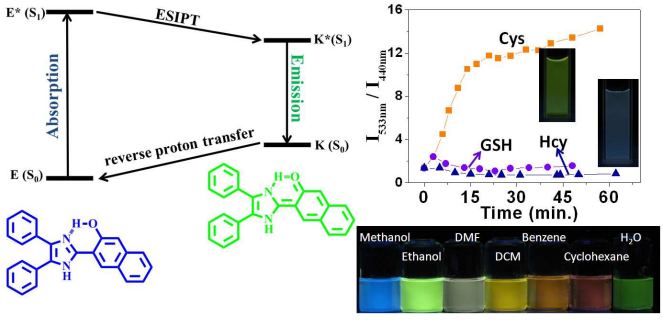

DPIN shows prominent ESIPT emission even in protic/ polar solvents, and further employed as sensor for selective detection of Cys.